INTERNATIONAL JOURNAL FOR NUMERICAL METHODS IN ENGINEERING
Int. J. Numer. Meth. Engng 2009; **80**:868–880
Published online 19 February 2009 in Wiley InterScience (www.interscience.wiley.com). DOI: 10.1002/nme.2564

A hybrid collocation/Galerkin scheme for convective heat transfer problems with stochastic boundary conditions

Paul G. Constantine*, †, Alireza Doostan and Gianluca Iaccarino

Institute for Computational and Mathematical Engineering, Stanford University, Stanford, CA 94305, U.S.A.

SUMMARY

We present a numerical method to study convective heat transfer in a high Reynolds number incompressible flow around a cylinder subject to uncertain boundary conditions. We exploit the one-way coupling of the energy and momentum transport to derive a semi-intrusive uncertainty propagation scheme, which combines Galerkin and collocation approaches for computing approximate statistics of the stochastic temperature field. The hybrid scheme converges rapidly and dramatically reduces the overall computational cost compared with the conventional uncertainty propagation schemes. Copyright © 2009 John Wiley & Sons, Ltd.

Received 9 August 2008; Accepted 23 December 2008

KEY WORDS: stochastic collocation; stochastic Galerkin; convective heat transfer

1. INTRODUCTION

The field of uncertainty quantification has blossomed in recent years with the introduction of provably accurate and easy-to-implement uncertainty propagation techniques for models—particularly differential equation models—with uncertain inputs. These uncertain inputs are modeled in a probabilistic framework and the propagation techniques allow the researcher to quantify the resulting uncertainty in the output quantities of interest by approximating their statistics, such as expectation, variance, and probability density functions. The propagation techniques can be classified into two categories: (i) *non-intrusive* techniques, such as standard Monte Carlo, employ preexisting deterministic tools as black box function evaluations, while (ii) *intrusive* techniques, such as polynomial chaos-based methods, require modifications to the mathematical and numerical formulation of the deterministic problem.

*Correspondence to: Paul G. Constantine, Institute for Computational and Mathematical Engineering, Stanford University, Stanford, CA 94305, U.S.A.
†E-mail: paul.constantine@stanford.edu

Contract/grant sponsor: DOE PSAAP

In flow simulation, the codes for deterministic problems are typically very complex with multiple models and tens to hundreds of input parameters. The challenge of writing new, *more* complex codes to solve non-deterministic problems is daunting; so, non-intrusive techniques are extremely attractive. However, intrusive implementations are often more accurate and provide more flexibility and efficiency for practical considerations such as grid refinement and memory management.

In this work, we examine the incompressible flow and heat transfer around an array of circular cylinders. In this case, the momentum transport is decoupled from the energy equations and this allows us to derive a *semi*-intrusive method combining the advantages of intrusive and non-intrusive methods. The physical model is based on the two-dimensional Reynolds-averaged Navier–Stokes (RANS) equations completed by an eddy-viscosity turbulence model [1]. We introduce stochastic boundary conditions to account for uncertainties in the incoming flow and the thermal state of the cylinder surface.

To approximate the statistics of the stochastic temperature field, we derive a hybrid uncertainty propagation scheme that applies (i) a spectral collocation method to the momentum equations and (ii) a spectral Galerkin method to the energy equation. The Galerkin form of the energy equation naturally decouples to a set of stochastic scalar transport equations, and the resulting system is developed within a commercial computational fluid dynamics code [2].

There has been a flurry of recent work applying both intrusive and non-intrusive techniques to stochastic flow models. We refer the curious reader to the following papers for further details [3–5]. General hybrid propagation methods are also not without precedent; see [6] for a similar approach that integrates spectral expansion methods with a collocation-like procedure for an efficient solution approach.

The paper is structured as follows: Section 2 describes the problem in full detail including our modeling choices for the uncertain input parameters and the specific objectives of our computations. Section 3 derives the hybrid propagation scheme for the model. Section 4 presents the results and analysis of our numerical experiments and Section 5 concludes with a summary and some recommendations based on our experience.

2. PROBLEM DESCRIPTION AND MOTIVATION

To achieve higher thermal efficiency and thrust, modern gas turbine engines operate at high combustor outlet temperatures and, therefore, turbine blades undergo severe thermal stress and fatigue. Secondary cooling flow passages are built into each blade (Figure 1) and consist of turbulators, film cooling holes, tube bundles, and pins. These are mostly used in the narrow trailing edge region of the blade [7].

In the present study we consider the flow and heat transfer around a periodic array of pins separated by a distance $L/D=1$ (where D is the cylinder diameter). The flow conditions are assumed to be fully turbulent with a Reynolds number based on the incoming fluid stream (and D) of $Re_D=1\,000\,000$. In this regime, direct solutions of the Navier–Stokes equations are impractical due to the range of length and time scales, which result in the extremely large computational cost; we resort to Reynolds-averaged modeling.

The problem is assumed to be two-dimensional and the computational domain is representative of a single row of aligned cylinders; $x_1 \in [-2, 10]$ and $x_2 \in [-2, 2]$ with a circle of radius 0.5 centered at the origin. Periodicity is enforced in the vertical direction with inflow and outflow conditions applied in the streamwise direction (see Figure 2).

DOI: 10.1002/nme

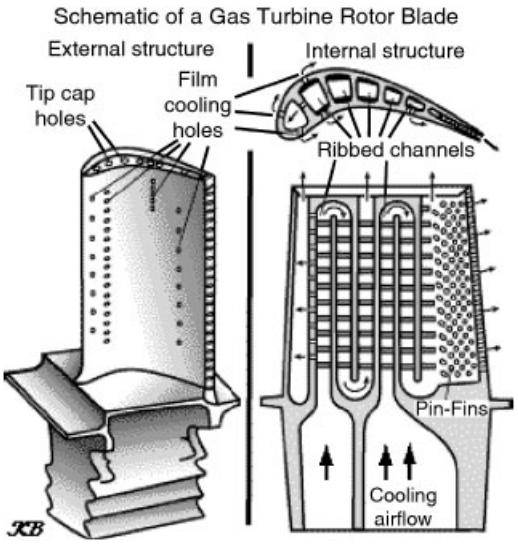

Figure 1. A turbine engine cooling system with a pin array cooling system.

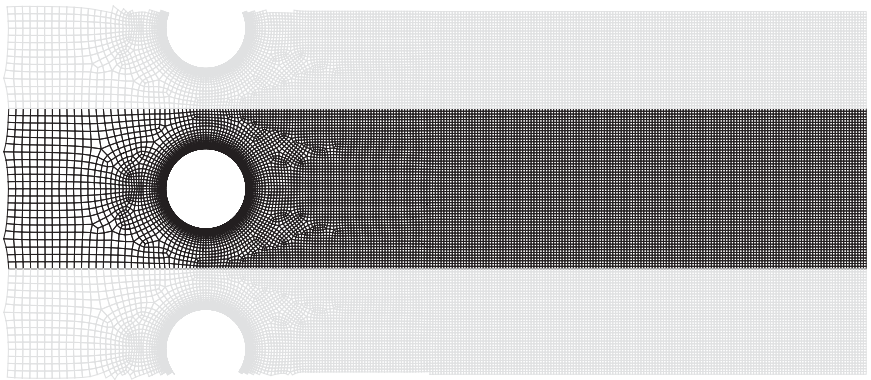

Figure 2. Computational mesh for two-dimensional cylinder problem.

Most numerical simulations of similar phenomena rely on simple thermal boundary conditions (constant temperature or constant heat flux) to evaluate the heat transfer characteristics of pin cooling devices. In realistic operating conditions, the overall surface thermal state is the result of an energy balance between convection and conduction in the fluid and in the solid. Therefore, accurate predictions of the heat transfer rates require the solution of the conjugate (solid–fluid) heat transfer problem. Instead of modeling the solid–fluid interactions directly [8], we introduce an uncertain heat flux on the boundary of the cylinder as a mild substitute; the precise formulation of this is given below.

Another simplification that is typically invoked in the design of blade cooling systems is to ignore the interactions between the various components (turbulators, slots, etc.) and optimize their

DOI: 10.1002/nme

performance independently. The pins, in particular, are the last stage of the cooling system and, therefore, more strongly affected by flow distortions introduced upstream. To investigate the effect of inflow perturbations, we model the uncertain inflow as a linear combination of oscillatory functions with different wave lengths and random amplitude; the precise formulation is given below.

2.1. Mathematical formulation

The governing equations are the two-dimensional RANS equations written in the assumption of incompressible fluid and steady flow. The conservation of mass, momentum, and energy can be written in indicial notation as

$$\frac{\partial U_i}{\partial x_i} = 0 \tag{1}$$

$$U_j \frac{\partial U_i}{\partial x_j} = \frac{\partial}{\partial x_j}\left[(\nu+\nu_t)\frac{\partial U_i}{\partial x_j}\right] - \frac{1}{\rho}\frac{\partial P}{\partial x_i} \tag{2}$$

$$U_j \frac{\partial T}{\partial x_j} = \frac{\partial}{\partial x_j}\left[\left(\kappa+\frac{\nu_t}{Pr_t}\right)\frac{\partial T}{\partial x_j}\right] \tag{3}$$

where the density (ρ), the molecular viscosity (ν), and the thermal conductivity (κ) are given properties of the fluid and assumed *constant*. The eddy viscosity (ν_t) is computed using the k-ω turbulence model [1], and the turbulent Prandtl number (Pr_t) is assumed to be a constant. In the assumption of incompressible flow, the energy equation is decoupled from the momentum equation and can be solved after the velocity field is computed.

2.2. Uncertainty sources

We assume that the sources of uncertainty are the specification of the velocity boundary condition on the incoming flow—the effect of the upstream components —and the definition of the thermal condition on the surface of the cylinder—the effect of the conductivity on the pin. Let Y_1, Y_2, and Y_3 be independent random variables on an appropriate probability space, each uniformly distributed over the interval $[-1, 1]$. The uncertain boundary conditions are prescribed by continuous functions of Y_i, $i = 1, 2, 3$, and are therefore random variables themselves.

We note here that by using a finite number of random variables to parameterize the uncertainty in the model (1)–(3), we introduce an *additional* coordinate space, i.e. the parameter space, which increases the number of dimensions in the problem. We then treat the parameter space much like the physical space in terms of discretization and solution procedures.

The inlet velocity profile is constructed as a linear combination of two cosine functions of $x_2 \in [-2, 2]$, i.e.

$$U|_{\text{inlet}}(x_2, Y_1, Y_2) = 1 + \sigma_1(Y_1 \cos(2\pi x_2) + Y_2 \cos(10\pi x_2)) \tag{4}$$

where σ_1 controls the inflow velocity fluctuations. For numerical experiments, we set $\sigma_1 = 0.25$, which ensured that the amplitude of the random fluctuations did not cause the inlet velocity

DOI: 10.1002/nme

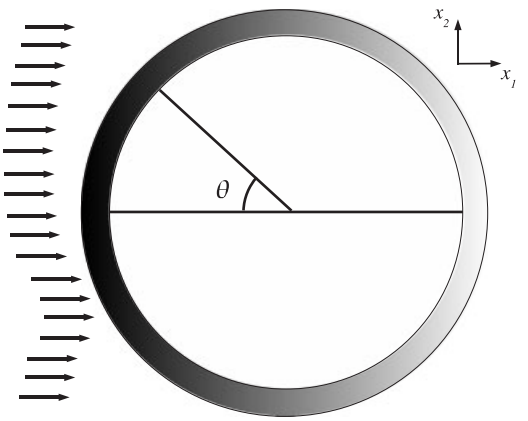

Figure 3. Schematic of uncertain inflow conditions. The arrows represent the stochastic inflow conditions and the shading represents the heat flux on the cylinder wall.

to become negative. This model allowed moderate random fluctuations (at most 25%) about a mean value, $\langle U_{\text{inlet}} \rangle = 1$ (where $\langle \cdot \rangle$ is the mathematical expectation operator). The wave numbers 2 and 10 in (4) were chosen to introduce low- and high-frequency fluctuations, respectively.

The heat flux is specified as an exponential function of Y_3 over the cylinder wall, namely

$$\left.\frac{\partial T}{\partial n}\right|_{\text{cyl}} (\theta, Y_3) = \mathrm{e}^{-(0.1+\sigma_2 Y_3)(\cos(\theta)/2)} \tag{5}$$

where n is the normal to the cylinder and σ_2 controls the influence of Y_3. The angle $\theta \in [0, \pi]$ is the angle away from the front of the cylinder as shown in Figure 3. For the numerical experiments, we chose $\sigma_2 = 0.05$. This model prescribes a larger heat flux at the left side of the cylinder where flow strikes it; the realization of Y_3 determines precisely how much greater. The maximum variability due to Y_3 is approximately 2.5%.

The one-way coupling in Equations (2) and (3) implies that the heat flux boundary condition parameterized by Y_3 has no affect on the velocity field. Therefore we can write $U_i = U_i(\mathbf{x}, Y_1, Y_2)$ for $i = 1, 2$. However, the temperature field *does* depend on the variability in the velocity inflow specification, which we denote by $T = T(\mathbf{x}, Y_1, Y_2, Y_3)$. This observation is crucial to the derivation of the hybrid method in Section 3.

Remarks

Our approach to modeling input uncertainties is admittedly ad hoc. For a real application—instead of a problem that is simply motivated by a real application—the parameters of a stochastic model would be estimated from experimental data, e.g. using a procedure such as [9].

2.3. Objective

We are interested in the effects of the input uncertainties on the temperature distribution around the cylinder wall. To this end, we desire the *variance* of temperature as a function of θ around

DOI: 10.1002/nme

cylinder. In other words, we wish to compute

$$\sigma_T^2(\theta) \equiv \mathbf{Var}[T|_{\text{cyl}}](\theta) = \langle (T|_{\text{cyl}}(\theta, Y_1, Y_2, Y_3) - \mu_T(\theta)) \rangle^2 \tag{6}$$

where $\mu_T(\theta) = \langle T|_{\text{cyl}} \rangle(\theta)$. To approximate σ_T^2, we use a hybrid stochastic Galerkin/collocation scheme described in the next section.

3. A HYBRID PROPAGATION SCHEME

The stochastic Galerkin method [10–12] approximates the stochastic output of a model by projecting it onto a global orthogonal polynomial basis, where the basis polynomials are functions of the parameterizing random variables. This technique has become very popular in uncertainty analysis communities for approximating moments and response surfaces of solutions to stochastic differential equation models. The details of this method have been presented in many excellent papers, and we refer the interested reader to the existing literature.

Stochastic collocation methods [13, 14], also known as the *probabilistic collocation methods* [15] or the *stochastic response surface methods* [16], similarly employ global basis polynomials to approximate the stochastic solution as a function of the parameterizing random variables. The primary difference between the two approaches lies in the choice of basis polynomial; the collocation methods employ a Lagrange interpolation basis, where the stochastic solution is evaluated at a discrete set of points within the parameter space. These points are typically chosen according to some interpolatory quadrature formula, e.g. the Gauss quadrature points. Again, we refer the reader to the existing literature for further details.

In general, the stochastic Galerkin method requires the solution of a large, coupled system of equations to solve for the coefficients of the global expansion. In contrast, the collocation method requires the evaluation of the stochastic model at a discrete set of points, similar to sampling methods such as Monte Carlo; thus, the collocation method can typically be implemented in a *non-intrusive* fashion. The difference in the approximation given by each approach, known as *aliasing error*, typically decays like the approximation error, i.e. exponentially fast, for linear problems [17].

In what follows, we apply a Galerkin method to the energy equation (3) and a collocation method to the non-linear momentum equation (2). A non-aliased Galerkin formulation of the full RANS equations would introduce a large, coupled system for the coefficients of the Galerkin approximation because of the non-linear convective operators in the momentum, the energy, and the turbulence transport equation. This greatly complicates the solution procedure and cannot be accomplished within the framework on a commercial CFD code. The present approach represents an attempt to retain an efficient Galerkin formulation for the (linear) energy transport while relying on a collocation formulation for the non-linear momentum equation. The result is a *semi*-intrusive hybrid scheme that takes advantage of the flexibility in the commercial software used to solve the flow problem.

Remark

The convergence of both Galerkin and collocation depend on the smoothness of the quantities of interest with respect to the random parameters. We assume that the relatively small and bounded range of variability in the boundary conditions ensures that the solution satisfies such a smoothness assumption.

DOI: 10.1002/nme

3.1. Galerkin method for the energy equation

To solve the Galerkin form of the energy equation (3), we express the Galerkin approximation of temperature T_N as an orthogonal expansion in Y_3:

$$T_N = T_N(\mathbf{x}, Y_1, Y_2, Y_3) = \sum_{k=0}^{N} T_k(\mathbf{x}, Y_1, Y_2)\psi_k(Y_3) \tag{7}$$

where the $\psi_k(Y_3)$ are the normalized Legendre polynomials. For notational convenience, we write this in vector notation as

$$T_N = \mathbf{T}^{\mathrm{T}}\Psi(Y_3) \tag{8}$$

where $\mathbf{T}$ is a vector of the expansion coefficients and $\Psi(Y_3)$ a vector of the Legendre basis polynomials. Then by projecting the energy equation onto each basis polynomial and requiring the residual to be orthogonal to the approximation space, we can write the Galerkin form as

$$\left\langle U_j \frac{\partial}{\partial x_j}(\mathbf{T}^{\mathrm{T}}\Psi(Y_3))\Psi(Y_3)^{\mathrm{T}} \right\rangle = \left\langle \frac{\partial}{\partial x_j}\left[\left(\kappa + \frac{\nu_t}{Pr_t}\right)\frac{\partial}{\partial x_j}(\mathbf{T}^{\mathrm{T}}\Psi(Y_3))\right]\Psi(Y_3)^{\mathrm{T}} \right\rangle \tag{9}$$

subject to the boundary conditions

$$\left\langle \frac{\partial}{\partial n}(\mathbf{T}^{\mathrm{T}}\Psi(Y_3))\Psi(Y_3)^{\mathrm{T}} \right\rangle\Big|_{\mathrm{cyl}} = \langle \mathrm{e}^{-(0.1+\sigma_2 Y_3)(\cos(\theta)/2)}\Psi(Y_3)^{\mathrm{T}} \rangle \tag{10}$$

Note that the projection is with respect to *only* Y_3. By the linearity of the expectation operator and the orthonormality of the basis, Equation (9) reduces to a set of *uncoupled* scalar transport equations for the coefficients of the Galerkin approximation T_N.

$$U_j \frac{\partial T_k}{\partial x_j} = \frac{\partial}{\partial x_j}\left[\left(\kappa + \frac{\nu_t}{Pr_t}\right)\frac{\partial T_k}{\partial x_j}\right], \quad k = 0, \ldots, N \tag{11}$$

each subject to boundary conditions on the cylinder wall given by

$$\frac{\partial T_k}{\partial n}\Big|_{\mathrm{cyl}} = \langle \mathrm{e}^{-(0.1+\sigma_2 Y_3)(\cos(\theta)/2)}\psi_k(Y_3) \rangle \tag{12}$$

(Recall that the subscript on U denotes the spatial coordinate while the subscript on T denotes the coefficient in the Galerkin expansion.) Note that the velocity components U_j and the temperature expansion coefficients T_k are functions of the spatial variables $\mathbf{x}$ and the random variables Y_1 and Y_2. Thus, by exploiting the one-way coupling in the RANS model, we have effectively replaced the random variable Y_3 by a set of $N+1$ stochastic transport equations. We can treat the new system of equations (momentum plus scalar transports) with a collocation method in *two* dimensions.

3.2. Collocation method for the modified system

Following the prescribed collocation algorithm, we evaluate the solution of the model (2) and (11) at a discrete set of points within the range of the random variables Y_1 and Y_2. We choose a tensor grid of Gauss–Legendre points with $M+1$ points in each direction. In other words we solve

DOI: 10.1002/nme

$(M+1)^2$ deterministic systems given by Equations (2) and (11), so that the stochastic solution is exact at each point $(\zeta_1^{(i)}, \zeta_2^{(j)})$, for $i, j = 0, \ldots, M$ in the two-dimensional Gauss–Legendre grid.

An important part of any implementation of a non-intrusive propagation technique is the deterministic solver. For each point $(\zeta_1^{(i)}, \zeta_2^{(j)})$, we employ the commercial software package Fluent [2] to solve for the temperature coefficients T_k and velocity fields U_1 and U_2 in the modified RANS equations. Fluent uses a finite volume second-order discretization on unstructured grids. The mesh has been generated to achieve high resolution of the boundary layer on the cylinder surface with $y^+ \approx 1$. We performed preliminary simulations to assess the resolution requirements for the present problem. Each deterministic solve is converged to steady state by ensuring that the residuals of all the equations are reduced by four orders of magnitude.

We are not interested in the response surface of the temperature as a function of Y_1, Y_2, and Y_3—only its variance. Therefore, we do not need to construct the interpolant through the collocation points. Instead we approximate the variance of temperature as a function of θ with the following steps:

1. For each point $(\zeta_1^{(i)}, \zeta_2^{(j)})$ in the tensor grid of Gauss–Legendre points, solve for the velocity field $U_1^{(i,j)}$ and $U_2^{(i,j)}$.
2. For $k = 0, \ldots, N$ solve the scalar transport equation for $T_k^{(i,j)}$ using the result from the velocity computation.
3. Compute the approximate variance of temperature as

$$\mu_T(\theta) \approx \sum_{i=0}^{M} \sum_{j=0}^{M} T_0^{(i,j)} w_{i,j} \equiv \bar{\mu}_T(\theta) \tag{13}$$

$$\sigma_T^2(\theta) \approx \sum_{i=0}^{M} \sum_{j=0}^{M} \left(\sum_{k=0}^{N} (T_k^{(i,j)}(\theta))^2 \right) w_{i,j} - \bar{\mu}_T(\theta)^2 \equiv \bar{\sigma}_T^2(\theta) \tag{14}$$

where $w_{i,j}$ is the weight corresponding to the Gauss–Legendre two-dimensional quadrature rule. This approximation follows from the variance formula (6) applied to the Galerkin approximation T_N.

3.3. Analysis of computational cost

The hybrid approach benefits both from the increased accuracy of the Galerkin formulation *and* decreased computational cost. In this section we compare the cost of the hybrid method with a naive three-dimensional collocation method. Let C_1 be the cost of one deterministic solve of the standard RANS equations (1)–(3) and let C_2 be the cost of the modified system (1), (2), and (11), (both solved with Fluent). Assume that

$$C_2 = \alpha(N) C_1 \tag{15}$$

where $\alpha(N) > 1$. The cost of naive three-dimensional collocation κ_c is then $C_1(M+1)^3$ and the cost of the hybrid method κ_h is $C_2(M+1)^2 = \alpha(N) C_1 (M+1)^2$. Thus we have the following relation:

$$\kappa_h = \frac{\alpha(N)}{M+1} \kappa_c \tag{16}$$

DOI: 10.1002/nme

In the numerical experiments in Section 4, we found that $N=4$ was sufficient for converged variance and $\alpha(4)\approx 2$. The M required for converged variance was 18. Therefore, the hybrid method is roughly 10 times as efficient as a naive three-dimensional collocation.

We note that if we had parameterized the stochastic heat flux boundary condition by *more* random variables to account for random spatial fluctuation, we expect the savings to be even greater.

4. RESULTS

In this section, we demonstrate numerical convergence of the approximate variance computed with the hybrid method, and we compare the results with a conventional Monte Carlo uncertainty propagation method. Following this verification, we make some remarks about the physical phenomenon described by the stochastic model.

4.1. Numerical convergence and verification

We first check the convergence of the variance approximation from the hybrid method by increasing (i) the order of the Galerkin approximation T_N and (ii) the number of points in the collocation scheme. Figure 4 displays the difference between the two-norm of the Galerkin approximations T_N and T_{N-1} on the cylinder wall for two-dimensional tensor collocation schemes built from the successive Gauss quadrature formulas. We set a tolerance of 10^{-5} to be consistent with the convergence tolerance for each Fluent solve. The approximation achieves the chosen tolerance when $N=3$ for each quadrature formula, and we include $N=4$ to increase the confidence in the convergence.

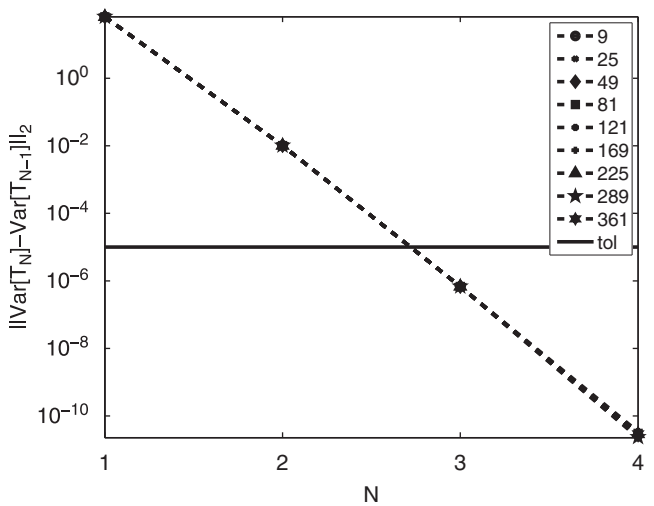

Figure 4. Convergence of the variance of the Galerkin approximation T_N as the number of terms in the expansion N increases. Each line represents the convergence for each quadrature rule. The convergence tolerance is 10^{-5}.

DOI: 10.1002/nme

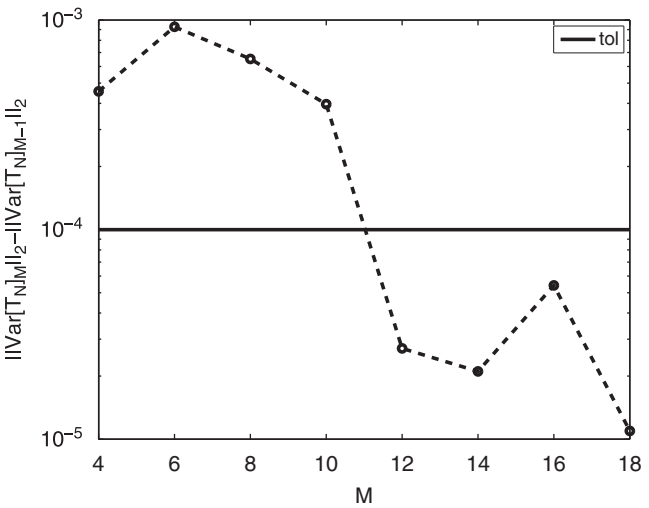

Figure 5. Convergence of the variance of the Galerkin approximation T_4 as the number of points in the quadrature rule M increases. The convergence tolerance is 10^{-4}.

From these results we conclude that $N=4$ is sufficient for converged results. We then check the convergence of the quadrature rule by increasing the number of points M. Note that the total number of points in the two-dimensional rule is $(M+1)^2$. We adjust the tolerance for the quadrature rule to 10^{-4} to account for the increased effects of rounding due to quadrature. In Figure 5, we plot the difference in the variance computed with an M point rule and an $M-1$ point rule. The values appear to converge after $M=10$, and we compute the remaining points to ensure that the results remain within the tolerance.

The relatively slow convergence of the quadrature versus Galerkin is not a result of any deficiencies in the method; the quadrature integrates along the random coordinates that affect the non-linear momentum equation. The non-linearity in the computation of velocity yields substantial error in the quadrature, which is absent in the Galerkin approximation of the linear energy equation.

4.2. A physical interpretation

In Figures 6 and 7 we plot the approximate expectation $\bar{\mu}_T$ and variance $\bar{\sigma}_T^2$ as a function of θ around the top half of the cylinder wall. We compare these results with a Monte Carlo method with 10 000 samples. The purpose of this comparison is to verify the qualitative features of the hybrid results, which fare very well.

In the expectation plot, the separation point of the flow is clearly identified by the sharp dip in the temperature. After the separation, the temperature rises again from the impact of the recirculating flow in the wake of the cylinder. The variance plot shows that the variability in temperature is largest at the front of the cylinder, i.e. the stagnation point of the flow. This results from two sources: first, the heat flux boundary condition (Equation (5)) is defined to have larger variability at the front of the cylinder; second, the variability in the inflow conditions (Equation (4)) affects the formation of a thermal boundary layer around the front of the cylinder wall; thus, modifying flow conditions at the stagnation point.

DOI: 10.1002/nme

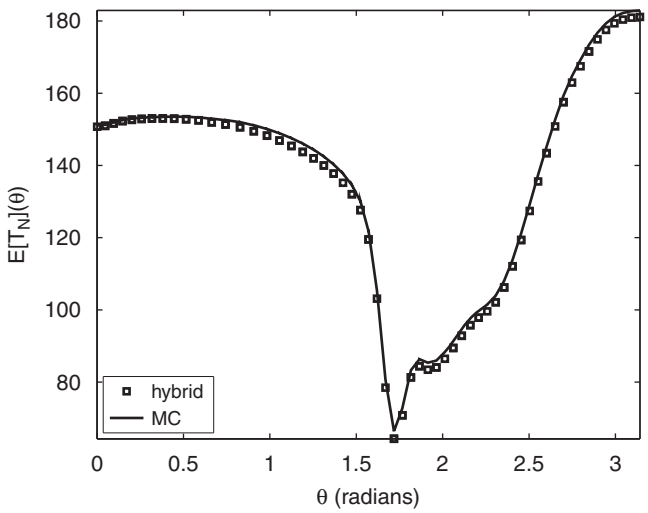

Figure 6. Approximate expectation as a function of θ around the cylinder wall computed with the hybrid method and the Monte Carlo method.

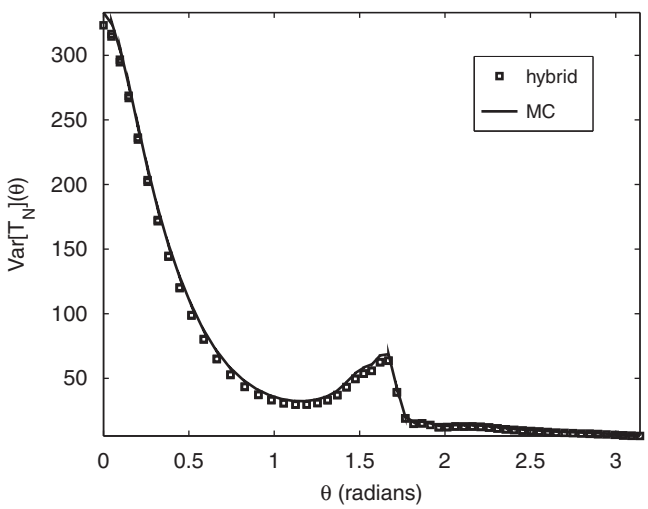

Figure 7. Approximate variance as a function of θ around the cylinder wall computed with the hybrid method and the Monte Carlo method.

In addition to a large temperature variance at the stagnation point, Figure 7 illustrates that the variability is considerably higher in the boundary layer upstream of the separation ($\theta \approx \pi/2$) than in the downstream area. This is expected since the variability in the upstream conditions does not directly *penetrate* the separated shear layer. In other words, the location of the flow separation is only a function of the Reynolds number that is not considerably altered by the different inflow conditions.

DOI: 10.1002/nme

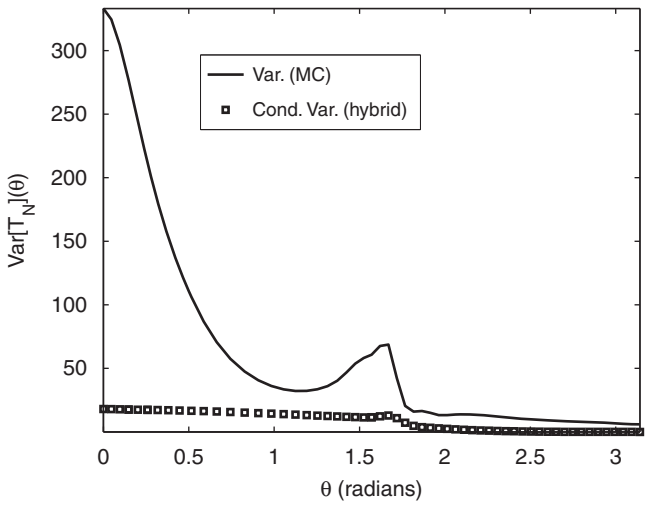

Figure 8. Approximate conditional variance at $Y_1 = Y_2 = 0$ as a function of θ around the cylinder wall computed with the hybrid method and the Monte Carlo method.

We can qualitatively assess the effects of the inflow variability on the variance at the stagnation point by approximating the *conditional* variance on the cylinder wall given $Y_1 = Y_2 = 0$. In fact, we have computed this quantity already when computed the solution corresponding to the central Gauss quadrature point ($\zeta_1 = 0, \zeta_2 = 0$). We approximate the conditional variance by

$$\mathbf{Var}[T(\mathbf{x}, Y_1, Y_2, Y_3) | Y_1 = Y_2 = 0] \approx \mathbf{Var}[T_N(\mathbf{x}, 0, 0, Y_3)] = \sum_{k=1}^{N} T_k(\mathbf{x}, 0, 0)^2 \tag{17}$$

In Figure 8 we plot the conditional variance against the Monte Carlo variance on the wall of the cylinder. We note that the conditional variance is much smaller than the Monte Carlo variance, which suggests that the total variance in temperature has *significant* contributions from the variability in Y_1 and Y_2.

5. SUMMARY

We have presented a semi-intrusive hybrid uncertainty propagation technique that combines stochastic collocation and stochastic Galerkin schemes to compute temperature statistics for the heat and fluid flow around an array of cylinders. The inflow velocity and the wall heat flux are assumed to be uncertain; we represent this uncertainty by a set of independent random variables. The one-way coupling between the momentum and energy equations implies that the uncertain heat flux has no effect on the velocity field. This allows us to represent the temperature using a polynomial expansion along only the random variables characterizing the heat flux. As a result we obtain a set of uncoupled stochastic scalar transport equations for the coefficients of the temperature expansion. The uncertainty in the velocity and Galerkin expansion coefficients is then treated using a *conventional* stochastic collocation approach. The hybrid method provides accurate, converged statistics *and* reduces the number of deterministic solves required. This method suggests

DOI: 10.1002/nme

avenues for developing hybrid methods in other multi-physics applications where the (random) input parameters selectively affect components of the system of interest.

REFERENCES

1. Menter FR. Zonal two equation k-w turbulence model predictions. *AIAA 93-2906*, 1993.
2. Fluent Inc. *FLUENT 6.1 Users Guide*. Lebanon, New Hampshire, 2003.
3. LeMaitre OP, Knio OM, Najm HN, Ghanem RG. A stochastic projection method for fluid flow. *Journal of Computational Physics* 2001; **173**:481–511.
4. Tartakovsky D, Xiu D. Stochastic analysis of transport in tubes with rough walls. *Journal of Computational Physics* 2006; **217**:248–259.
5. Asokan BV, Zabaras N. Using stochastic analysis to capture unstable equilibrium in natural convection. *Journal of Computational Physics* 2005; **208**:134–153.
6. Ghanem R. Hybrid stochastic finite elements and generalized Monte Carlo simulation. *Journal of Applied Mechanics—Transactions of the ASME* 1998; **65**:1004–1009.
7. Lyall M. Heat transfer from low aspect ratio pin fins. *Master's Thesis*, Virginia Polytechnic Institute and State University, June 2006.
8. Iaccarino G, Ooi A, Durbin PA, Behnia M. Conjugate heat transfer predictions in two-dimensional ribbed passages. *International Journal of Heat and Fluid Flow* 2002; **23**:340–345.
9. Ghanem R, Doostan A. On the construction and analysis of stochastic models: characterization and propagation of the errors associated with limited data. *Journal of Computational Physics* 2006; **217**:63–81.
10. Ghanem R, Spanos P. *Stochastic Finite Elements*: *A Spectral Approach*. Springer: New York, 1991.
11. Xiu D, Karniadakis G. The Wiener–Askey polynomial chaos for stochastic differential equations. *SIAM Journal on Scientific Computing* 2002; **24**:619–644.
12. Babuska I, Tempone R, Zouraris GE. Galerkin finite element approximations of stochastic partial differential equations. *SIAM Journal on Numerical Analysis* 2004; **42**(2):800–825.
13. Babuska I, Nobile F, Tempone R. A stochastic collocation method for elliptic partial differential equations with random input data. *SIAM Journal on Numerical Analysis* 2007; **45**:1005–1034.
14. Xiu D, Hesthaven JS. High order collocation methods for differential equations with random inputs. *SIAM Journal on Scientific Computing* 2005; **27**:1118–1139.
15. Loeven GJA, Witteveen JAS, Bijl H. Probabilistic collocation: an efficient non-intrusive approach for arbitrarily distributed parametric uncertainties. *Proceedings of the 45th AIAA Aerospace Sciences Meeting and Exhibit*, *AIAA Paper 2007-317*, Reno, January 2007.
16. Isukapelli SS, Roy A, Georgopoulos PG. Efficient sensitivity/uncertainty analysis using the combined stochastic response surface method and automated differentiation: application to environmental and biological systems. *Risk Analysis* 2000; **20**(5):591–602.
17. Canuto C, Hussaini MY, Quarteroni A, Zang T. *Spectral Methods*: *Fundamentals in Single Domains*. Springer: Berlin, 2006.

DOI: 10.1002/nme